Fatigue Crack Propagation Properties in SAC 50 Structural Steel Welded Joints

Geraldo de Paula Martins[1], Jefferson José Villela[1], Emerson Giovani Rabello[1] Carlos Alberto Cimini Jr.[2], and Leonardo Barbosa Godefroid[3]

[1]Researcher of Nuclear Technology Development Center/Nuclear Energy National Commission, Belo Horizonte, Minas Gerais, Brazil
[2]Professor of Mechanical Engineering Department/Federal University Minas Gerais. Belo Horizonte, Minas Gerais, Brazil
[3]Professor of Metallurgical Engineering Department/Federal University of Ouro Preto, Ouro Preto, Minas Gerais, Brazil

ABSTRACT

In this work fatigue crack propagation resistance was studied by using compact tension specimens of SAC 50 structural steel welded joints with 12 mm and 19 mm in thickness. Hardness measurements at superficial and transversal through thickness on the Base Metal (BM), Heat Affected Zone (HAZ) and Melted Zone (MZ) were made and the results were compared with the yield stress in each one of the three regions. From this, a relationship between hardness and yield stress was obtained. Fatigue crack propagation tests were accomplished using specimens with notch located at the BM, HAZ and MZ. Some specimens were submitted to stress relief heat treatment (SRHT) before fatigue crack propagation tests. It was observed a compression residual stress relieve at HAZ. Some propagation crack models were compared for three specimens, one of the BM, other with notch localized on the HAZ and one with the notch localized on the MZ. It was concluded that the models, which reach all the three regions of crack growth rate fit well to data

Keywords: fatigue crack propagation, fracture, welded joints, heat affected zone, melted zone

INTRODUCTION

Several welded structures are sometimes submitted to fatigue when in service. Due to technological developing, the metallic structures manufacturers had claimed steels with mechanical and environmental corrosion resistance moreover good weldability. From these requirements the steels manufacturers had presented at the commerce low alloy steels, with high and mean mechanical resistance, weldable and with high atmospheric corrosion. The SAC 50 steels manufactured verify these requirements. Such steels have the property of develop a compact oxide layer at the surface that is adherent to the metallic substrate when exposed to industrial environmental medium. The higher resistance of these steels enable a substantial reduction in weight because of the small thickness, resulting as a consequence in economy of weld, transportation and so on. The higher resistance in atmospheric corrosion results in a higher durability of the structure. The utilization of adequate filler metals allow also to assure an atmospheric corrosion resistance at the welded joints, by the obtention of a weld metal with the same properties of the base metal.

Fatigue Crack Propagation

Fatigue crack propagation makes use of the fracture mechanic concepts, in special the stress intensity factor range presented bellow.

Some definitions used in fatigue are presented from a plat submitted to cyclic stress containing a through crack, these stresses varying between a maximum and minimum value (Fig. 1)

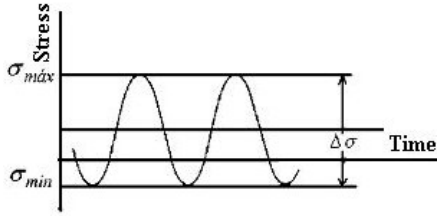

Fig. 1 Cyclic stress parameters with constant amplitude

The principal parameters are defined bellow:
stress range:

$$\Delta\sigma = \sigma máx - \sigma min \tag{1}$$

stress intensity factor range:

$$\Delta K = K_{max} - K_{min} = \Delta\sigma\sqrt{\pi a} f\left(\frac{a}{W}\right) \tag{2}$$

stress amplitude:

$$\sigma_a = \frac{\sigma_{max} - \sigma_{min}}{2} \tag{3}$$

mean stress:

$$\sigma_m = \frac{\sigma_{max} + \sigma_{min}}{2} \tag{4}$$

stress ratio:

$$R = \frac{\sigma_{min}}{\sigma_{max}} \tag{5}$$

For R=-1, the stresses are reverted and $\sigma_{min} = -\sigma_{max}$
The fatigue crack propagation rate is defined as the crack extension rate, Δa, by the number of cycles ΔN, that is, Δa/ΔN and

$$\lim_{\Delta N \to \infty} \frac{\Delta a}{\Delta N} = \frac{da}{dN} \tag{6}$$

For $R=\sigma_{min}/\sigma_{max}$=constant, ΔK correlates crack propagation rate in specimens with different stress rates and crack lenghs in specimens with different geometry.

Several equations describing the behavior of the crack propagation were proposed. Such equations involve constants of the material, loading rate and applied stress level. The main equations are presented bellow [1]
Paris model: Paris [2] and Paris & Erdogan [3] were the first to find a relationship type power law to describe the fatigue crack propagation at the region II [3]. They proposed an empirical relationship Eq. (7) where C and n are constants of the material, experimentally determined:

$$\frac{da}{dN} = C\,(\Delta K)^n \tag{7}$$

Priddle model: Priddle [4] developed a relationship valid for I, II and III regions, where the value of ΔK_{th} is dependent of R. C and n are constants of the material.

$$\frac{da}{dN} = C\left(\frac{\Delta K - \Delta K_{th}}{K_c - K_{max}}\right)^n \tag{8}$$

Colliepriest model [5]: a proposed relationship type hyperbolic tangent valid for the tree regions I, II and III.

$$Log\left(\frac{da}{dN}\right) = C_1 + C_2 \operatorname{arctgh}\left[\frac{Log\left(\frac{\Delta K^2}{K_{th} K_c (1-R)^2}\right)}{Log\left(\frac{K_c}{K_{th}}\right)}\right] \tag{9}$$

C_1 and C_2 are parameters to be determined, for each material; K_c is the critical value and K_{th} is the threshold value of K.

METHODOLOGY

The material used in this work is the structural material, employed in buildings, bridges and other applications, USI-SAC 50 , 12mm and 19mm in thickness. The chemical composition is presented in the Tab 1.

The welding process used were the shielded metal arc welding (SMAW), with preparation in bevels V and ½ V. Bevel V preparation for specimens with notch localized on the MZ and bevel ½ V preparation for specimens with notch localized on the HAZ. After welding, the weld joints were removed specimens for fatigue crack propagation tests according Fig. 2:

Some specimens were submitted to stress relieve heat treatment, and submitted to Vickers hardness measurements before and after SRHT. The purpose is to observe the influence of the SRHT on the fatigue crack propagation.

Table 1: Chemical composition of the USI-SAC 50, furnished by the manufacture

Thickness (mm)	Element											
	C	S	Mn	P	Si	Cr	Ni	Cu	Ti	Nb	V	N (ppm)
12	0.12	0.013	1.15	0.024	0.30	0.45	0.18	0.29	0.00	0.030	0.010	53
19	0.11	0.013	1.13	0.024	0.33	0.44	0.18	0.27	0.01	0.010	0.005	53

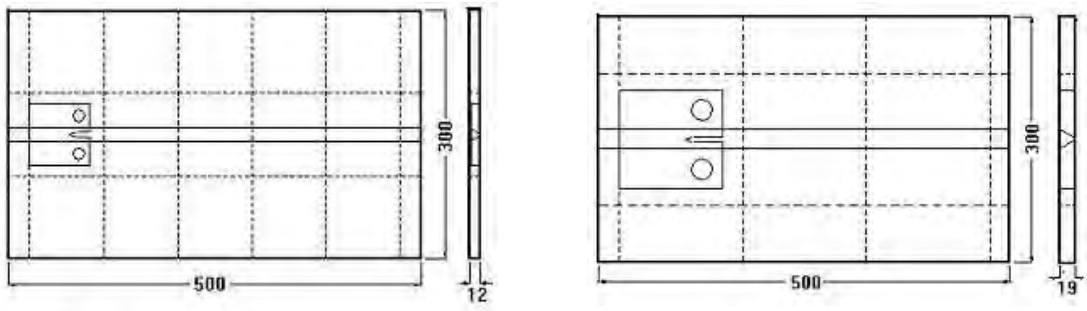

Figure 2: Removed of fatigue crack propagation test specimens (Scheme) (a) 12mm thickness; (b) 19mm thicknes

The specimens for fatigue crack propagation tests were prepared according ASTM E 647 [6] and are schematized on Fig 3 for 12mm and 19mm in thickness.

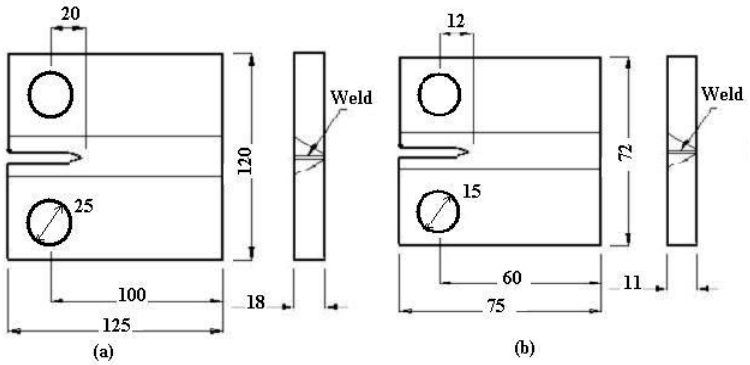

Figure 3: Scheme of the specimens for fatigue crack propagation tests: (a) 19mm weld joints; (b) 12mm weld joints

Fatigue Crack Propagation Tests

Crack propagation tests were accomplished in CT specimens from BM and welded joints and the notch of the welded joint specimens were localized at the HAZ and MZ with T-L orientation. Some welded joint specimens were tested AW and others were tested after SRHT. After this, a Paris equation was adjusted for all specimens tested, from the data obtained. The coefficients C and n for the adjustment of the logarithmic equation were obtained from the software EXCEL using Regression Analyses.

For comparison, the Priddle and Collipriest models of fatigue crack propagation were studied and compared.

RESULTS

The mean values of yield stress and ultimate stress of the welded joints were obtained by Martins [7] and are presented on the Tab.2:

Table 2: Mean values of mechanical properties of USI-SAC 50 welded joints stress

Thickness (mm)	Orientation	0.2% Yield stress (MPa)	Ultimate stress (MPa)
12	Longitudinal	537.33 ± 14.34	681.33 ± 8.25
	Transverse	480.00 ± 8.16	597.67 ± 8.16
19	Longitudinal	583.33 ± 12.81	652.00 ± 12.03
	Transverse	403.00 ± 4.97	546.33 ± 6.34

Hardness Results

The localization of hardness measurements Hv at the conditions AW and with SRHT is showed on Fig. 4. The mean and standard deviation are presented on Table 3.

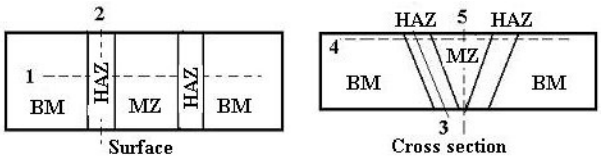

Figure 4: Localization of hardness measurements on the welded joints 12mm and 19mm in thickness.

Table 3: Mean values of hardness measurements of the welded joints

Hardness mean value (Hv); load: 98 N							
Thickness		12 mm			19 mm		
Region		BM	HAZ	MZ	BM	HAZ	MZ
Condition	AW	212.0±9.1	252.0±18.3	298.9±32.7	190.4±15.2	248.3±16.2	228.3±33.2
	SRHT		230.0±25.9	239.7±16.2		212.4±6.3	220.9±9.2

The hardness measurements on the HAZ revealed values higher than the corresponding to the values of BM and MZ. It is probably due to the dimensions of the identator to be inferior to the corresponding values of microhardness in smaller grains containing carbides. Microhardness measurements were made also in specimens polished of 12mm and 19mm welded joints and the results are presented on the Tab. 4.

Table 4: Mean values of microhardness measurements of the welded joints

Microhardness mean values (Hv); load: 0.98N		
Region	Thickness (mm)	
	12	19
	Mean ± Standard deviation	Mean ± Standard deviation
BM	177.31 ± 5.38	168.18 ± 9.15
HAZ	203.13 ± 13.98	221.16 ± 31.45
MZ	213.87 ± 6.50	249.40 ± 27.81

From Tab 3 and Tab 4 we can observe a decreasing of hardness after SRHT. The mean values of yield stress and hardness obtained for the three regions (BM, HAZ and MZ), and using also the values obtained by Alcântara [8] respectively σ_y=442,9±7,8 MPa (12mm in thickness) and σ_y=415,2±31.8 MPa (19mm in thickness) for the BM, can be compared with the corresponding mean hardness (and microhardness) obtaining an empirical formula Eq.10:

$$\sigma_y = 2.25Hv \quad (10)$$

The suggested relation (Eq. 10) , for values of hardness and yield stress experimentally obtained presents a maximum variation of 20%. It can be considered a good empirical relation.

Fatigue Crack Propagation Results

The curves da/dN x ΔK_{eff} of the 12mm and 19mm in thickness specimens obtained from fatigue crack propagation tests according ASTM E 647 [6] are presented on Fig. 5

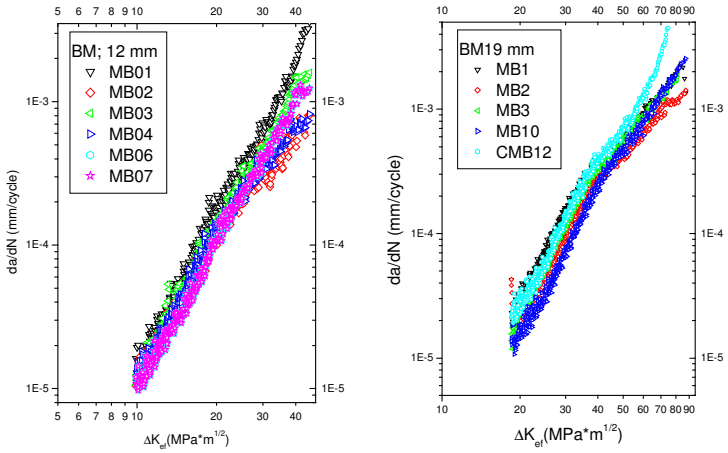

(a) (b)

Figure 5: Graphic of da/dN x ΔK_{eff}, BM specimens; (a) 12mm in thickness plate R=0.1; amplitude 3.6kN; (b) 19mm in thickness plate; R=0.1; amplitude 7.7 kN

The values of ΔK_{eff} were determined from the relationship proposed by Kumar and Singh [9], due to crack closed phenomena. For some specimens it can be observed a small retard on the crack propagation rate corresponding to values of ΔK_{eff} between 30 and 40 MPa$\sqrt{m}$. This is due, probably, to variations in microstructure on the orientation transverse to the rolling direction, that, according Lal [10] involves plastic deformation, stress ratio and Young modulus combination.

On the Fig 6 is presented da/dN x ΔK_{eff} graphics of the specimens Z2, Z3, AW, and Z5, Z6 with SRHT (12mm plate), with notch located on the HAZ and in the Fig 7 is presented da/dN x ΔK_{eff} graphics of the specimens ZTA1, ZTA2 and ZTA3, AW, and ZTA4, ZTA5 and ZTA6, with SRHT (19mm plate).

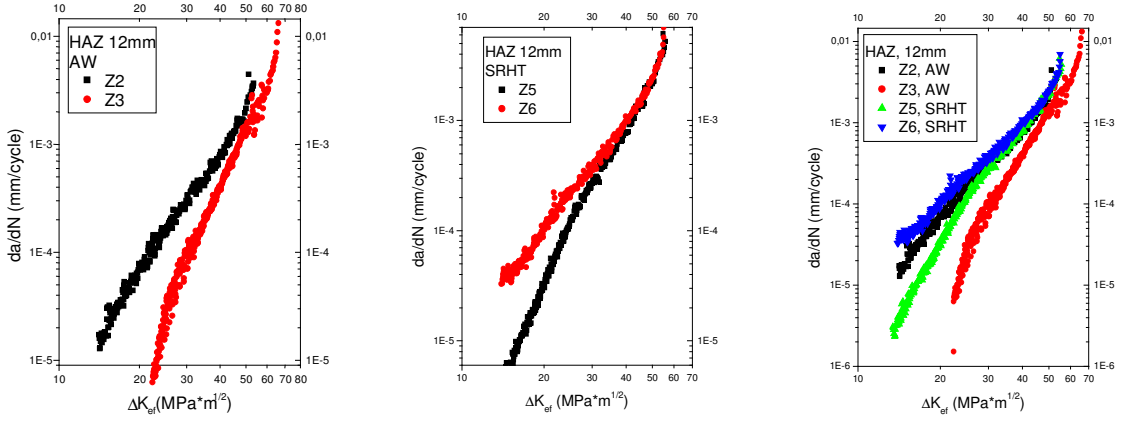

(a) (b) (c)

Figure 6: Graphic of da/dN x ΔK_{eff}, 12mm in thickness plate R=0.1 amplitude 4.6kN; (a) Z2, Z3 specimens; AW; (b) Z5, Z6 specimens, SRHT; (c) Z1, Z2, Z5 and Z6 specimens

On Fig 7 it can be observed a retardation on the crack propagation rate corresponding at the value near of 60 MPa$\sqrt{m}$. It can be probable to the existence of compressive residual stresses at the tip crack propagation. This phenomena is more evident on ZTA3 specimen, tested on the condition AW. This specimen showed a higher resistance to crack propagation.

The specimens that were submitted to SRHT showed a crack propagation rate more uniform. After the SRHT the compression residual stress were redistributed.

On Fig. 8 is presented da/dN x ΔK_{eff} graphics of the specimens F01, F07 AW, and F13, F14 and F15, with SRHT (12mm plate), with notch located on the MZ.

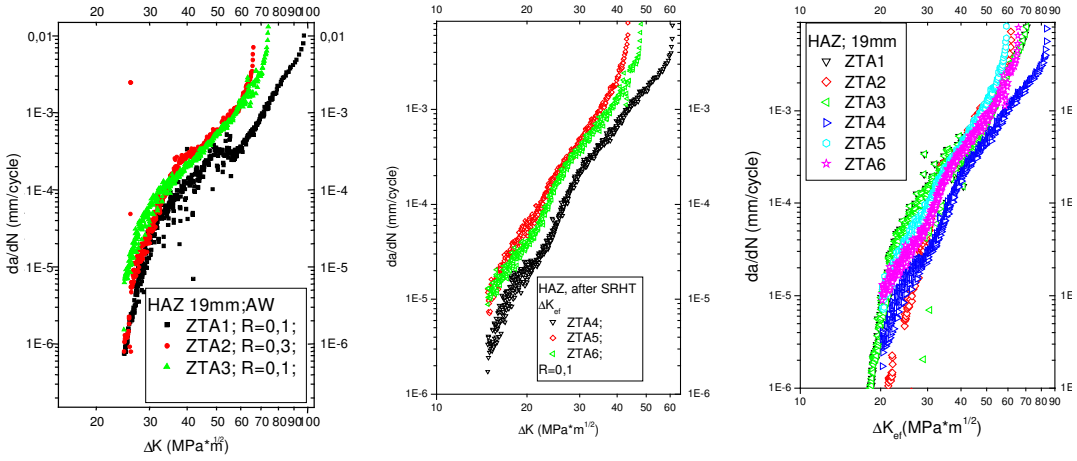

(a) (b) (c)

Figure 7: Graphic of da/dN x ΔK_{eff}, 19mm in thickness plate R=0.1 amplitude 11.8kN; (a) ZTA1, ZTA2 and ZTA3 specimens; AW; (b) ZTA4, ZTA5 and ZTA6 specimens, SRHT; (c) Z1, Z2, Z5 and Z6 specimens

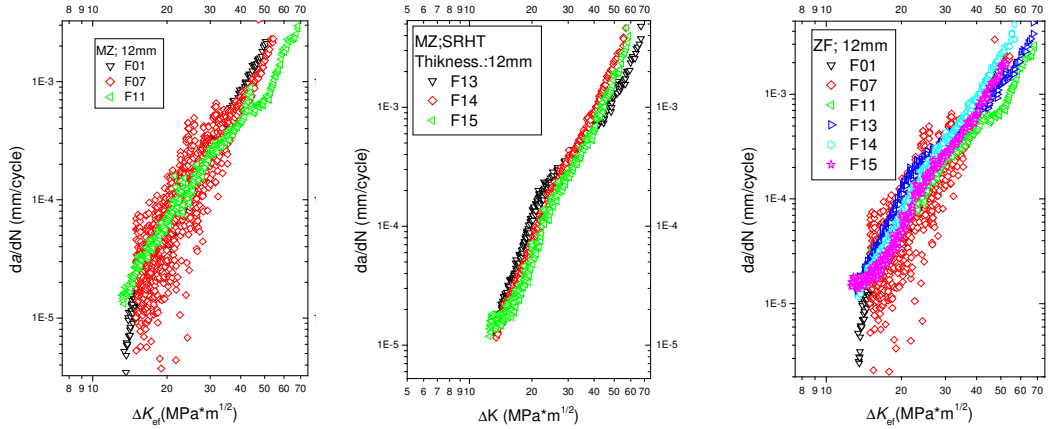

(a) (b) (c)

Figure 8: Graphic of da/dN x ΔK_{eff}, 12mm in thickness plate R=0.1 amplitude 4.6kN; (a) F01, F07 and F11 specimens; AW; (b) F13, F14 and F15 specimens, SRHT; (c) F01, F07, F11, F13, F14 and F15 specimens

It can be observed that the specimens with notch localized at the MZ that were submitted to SRHT showed a smaller crack propagation rate. Probably, there were tension residual stresses before the SRHT, and after the SRHT these tension residual stresses were reduced.

Determination of the Coefficients and exponents from Regression Analyses

The coefficients (C) and exponents (n) of the Paris equation were determined from regression analyses using the data obtained on the crack propagation tests, with 95% confidence. From Eq. 9,

$$\mathrm{Log}\left(\frac{da}{dN}\right) = \mathrm{Log}(C) + n\mathrm{Log}(\Delta K) \tag{11}$$

Equation type Y=A+nX

From analyses of variance, the coefficients C can be obtained and from A and n is obtained directly from the analysis. The results are presented on the Tab. 5.

Table 5: Coefficients *C* and exponents n of Paris equation, with 95% confidence limit

Groups	Coefficient *C*			n		
	Mean	95% Inferior	95% Superior			
MB12	4.487×10^{-9}	4.235×10^{-9}	4.753×10^{-9}	3.430	3.411	3.450
MB19	6.694×10^{-9}	6.148×10^{-9}	7.288×10^{-9}	3.183	3.156	3.209
Z12(CS)	1.120×10^{-9}	6.856×10^{-10}	1.903×10^{-9}	3.486	3.330	3.642
Z12(TTAT)	8.963×10^{-10}	6.121×10^{-10}	1.313×10^{-10}	3.742	3.624	3.859
ZTA19(CS)	3.337×10^{-13}	1.773×10^{-13}	6.281×10^{-13}	5.616	5.439	5.794
ZTA19(TTAT)	1.082×10^{-11}	9.671×10^{-12}	1.190×10^{-11}	4.882	4.851	4.913
ZF12(CS)	4.999×10^{-9}	4.093×10^{-9}	6.105×10^{-9}	3.164	3.102	3.226
ZF12(TTAT)	1.595×10^{-9}	1.395×10^{-9}	1.823×10^{-9}	3.559	3.518	3.601

Comparison of Crack Propagation Models

The Paris model applies only at the region II of the da/dN x ΔK curve. As a consequence, if the curve presents data at the region I, the Paris model is very conservative, because on the region I the crack propagation rate is very small. On Fig. 9 is presented three graphics of the specimens BM01, Z5 and F01 from 12mm plate. On these graphics are also plotted the curves corresponding to Priddle model and Collipriest model, with the straight line corresponding to Paris model. The correspondent equations are presented on Tab. 6.

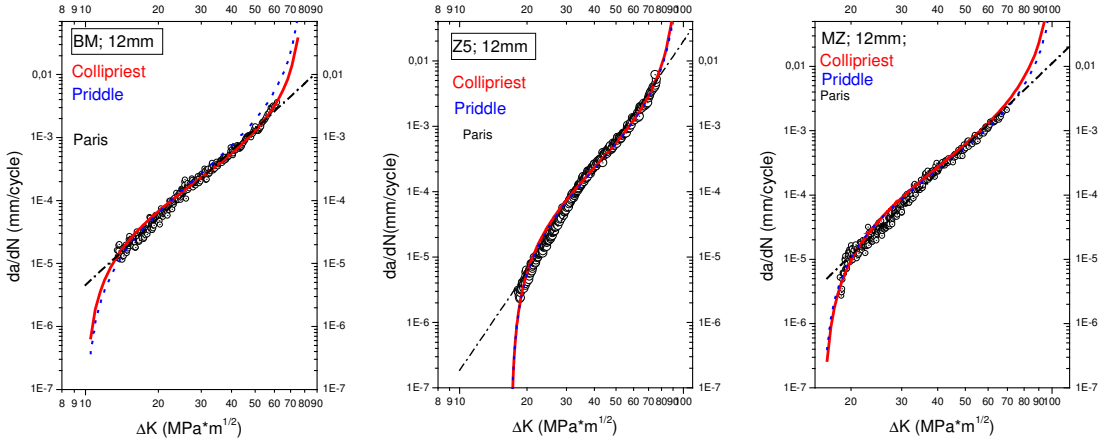

(a) (b) (c)

Figure 9: Crack propagation models (a) specimen BM01; (b) specimen Z5; (c) specimen F01

Table 6: Equations of fatigue crack propagation, according some models

Model	Region		
	BM	HAZ	MZ
Paris	$\frac{da}{dN} = 3{,}94 \times 10^{-9} \times (\Delta K)^{3{,}54}$	$\frac{da}{dN} = 5{,}5 \times 10^{-9} \times (\Delta K)^{3{,}82}$	$\frac{da}{dN} = 1{,}17 \times 10^{-10} \times (\Delta K)^{4{,}28}$
Collipriest ÷	$\mathrm{Log}\left(\frac{da}{dN}\right) = -3{,}71 + 1{,}33 \times \tan^{-1}\mathrm{h}\left[\frac{\mathrm{Log}\left(\frac{\Delta K^2}{800}\right)}{\mathrm{Log}(8)}\right]$	$\mathrm{Log}\left(\frac{da}{dN}\right) = -3{,}62 + 1{,}43 \times \tan^{-1}\mathrm{h}\left[\frac{\mathrm{Log}\left(\frac{\Delta K^2}{1621}\right)}{\mathrm{Log}(5{,}6)}\right]$	$\mathrm{Log}\left(\frac{da}{dN}\right) = -3{,}55 + 1{,}48 \times \tan^{-1}\mathrm{h}\left[\frac{\mathrm{Log}\left(\frac{\Delta K^2}{1642}\right)}{\mathrm{Log}(6{,}41)}\right]$
Priddle	$\frac{da}{dN} = 1{,}41 \times 10^{-3} \times \left(\frac{\Delta K - 8}{88 - K_{máx}}\right)^{1{,}636}$	$\frac{da}{dN} = 1{,}08 \times 10^{-3} \times \left(\frac{\Delta K - 17}{106 - K_{máx}}\right)^{1{,}592}$	$\frac{da}{dN} = 1{,}28 \times 10^{-3} \times \left(\frac{\Delta K - 16}{114 - K_{máx}}\right)^{1{,}536}$

From numerical integration were made calculations of the cycle numbers using the three models of the Tab. 6 and the correspondent values were compared with the real number of cycles for the specimens F01 and Z5, obtained on the tests. The results obtained are presented on Tab 7:

Table 7: Number of cycles obtained from the tests and from numerical integration f the three equations (Paris, Priddle and Collipriest)

Specimen	Tests	Models		
		Paris	Priddle	Collipriest
Z5	827000	184001	766705	827612
F01	1410000	232973	1429033	1415472

As can be observed, the Paris model is very conservative. The Priddle and Collipriest models presented results very near to the real data and the Collipriest model is the most real.

CONCLUSIONS

The hardness results measurements in the HAZ and MZ were higher than the results obtained from the BM.

Comparison of mean hardness measured with the yield stresses for the three regions allow to establish a correlation between hardness and yield stress, the relationship obtained were $\sigma_y = 2.25$ HV.

From fatigue crack propagation results it was observed that the specimens with notch localized on the BM is more homogeneous and the specimens AW with notch localized on the HAZ presented more dispersion and after SRHT the results were more homogeneous.

The comparison of fatigue crack propagation models with real data, the Priddle and Collipriest models adjusted well with the data, the Collipriest model presenting the best adjustment.

REFERENCES

1. Godefroid, L. B., Cândido, L. C. and Moraes, W. W., 2004. "Análise de Falhas". Curso da ABM. 30 de agosto a 03 de setembro de 2004. Belo Horizonte, MG.
2. Paris, P. C., Gomes, M. P., and Anderson, W. P., "A Rational Analytic Theory of Fatigue". The Trend in Engineering, Vol. 13, 1961, pp. 9-14.
3. Paris, P. C. and Erdogan, F., "A Critical Analysis of Crack Propagation Laws." Journal of Basic Engineering, Vol. 85, 1960, pp. 528-534
4. Priddle, E. K., 1976. "High Cycle Fatigue Crack Propagation Under Random and Constant Amplitude Loadings." International Journal of Pressure Vessels and Piping, 4, pp. 89-117.
5. Barroso, E. K. L.,. "Efeito da Pré-deformação e Shot Peening na Tenacidade à Fratura e Propagação de Trinca por Fadiga da Liga de Alumínio 7475-T7351, da Aplicação Aeronáutica." Dissertação de Mestrado. Universidade Federal de Ouro Preto. Programa de Pós Graduação em Engenharia de Materiais. Ouro Preto, MG, Brasil, 2004.
6. ASTM E 647 "Standard Method for Measurement of Fatigue Crack Growth Rates." Philadelphia, 2000.
7. Martins, G. P. "Tenacidade à Fratura e Propagação de Trinbcas em Juntas Soldadas de Aço Estrutural Resistente à Corrosão Atmosférica." Tese de Doutorado. Departamento de Engenharia Mecânica, Universidade Federal de Minas Gerais, Belo Horizonte, Minas Gerais, 2004, 203 p.
8. Alcântara, F L. de,. "Comportamento do Crescimento de Trinca por Fadiga de um Aço do Tipo USI-SAC-50 Laminado a Quente em Diferentes Espessuras." Dissertação de mestrado. Pontifícia Universidade Católica de Minas Gerais. Belo Horizonte, MG, 2003.
9. Kumar, R.; Singh, K.,. "Influence of Stress Ratio on Fatigue Crack Growth in Mild Steel." Engineering Fracture Mechanics, vol. 50, N° 3, 1995, pp. 377-384.
10. Lal, D. N., "A New mechanistic Approach to Analyzing LEFM Fatigue Crack Growth Behavior of Metals and Alloys." Engineering Fracture Mechanics, vol. 47, nº 3, pp. 379-401, 1994.